Ultra-Wideband Virtual Impedance Circuit for Grid-Connected Inverter

Riki Yamazaki[1], Hiroki Watanabe[1], Jun-ichi Itoh[1], Keisuke Kusaka[1]

[1] Nagaoka University of Technology

Abstract – Passive components of power conversion systems (PCSs) are desired to have a small volume to increase power density. A virtual impedance circuit, consisting of a small inductor and an inverter, can be connected in series or parallel to conventional PCSs, capable of replacing a bulky passive component. However, the conventional virtual impedance circuit is designed to be driven at low-switching frequencies, limiting miniaturization efforts on inductor size. This paper proposes an ultra-wideband virtual impedance circuit for the inductor of a grid-connected inverter. The external circuit operating at a high-switching frequency in the proposed virtual impedance absorbs only the current ripple, thus behaving as an additional inductor. Furthermore, the validity of the proposed circuit is experimentally demonstrated using an 800-W prototype.

Keywords power conversion system, grid-connected inverter, interconnected inductor, virtual impedance circuit

I. Introduction

In recent years, photovoltaic systems (PVs) have been actively researched due to the increasing demand for renewable resources. In general, PVs require power conversion systems (PCSs) consisting of a single-phase grid-connected inverter. In order to increase the power density of PCSs, downsizing the interconnected inductor in the inverter is required. By reducing the inductance with the high switching frequency of the inverter, it is possible to reduce the volume of the inductor. However, the reduction in inductance leads to a decrease in the disturbance suppression performance of the current controller, which undesirably increases the THD of output current.

As an alternative inductor downsizing method, a virtual impedance circuit, consisting of a small inductor and an inverter operating at a high-switching frequency, capable of replacing a bulky passive inductor, has been proposed. The grid-connected inverter as shown in Fig. 1 has been suggested by virtually varying the inductance [1]. However, the series-type virtual impedance circuit increases power losses as the entire line current flows through the external circuit. Moreover, the conventional virtual impedance circuit is designed to be driven at switching frequencies of several tens of kHz, and the control bandwidth is narrow.

This paper proposes a novel virtual impedance circuit topology, which behaves as an additional inductor for a grid-connected inverter. This external circuit operating at a high-switching frequency in the virtual impedance absorbs only the current ripple. The validity of the proposed system is experimentally demonstrated using an 800-W prototype.

II. Proposed virtual impedance circuit

Fig. 2 shows the concept of the proposed virtual impedance circuit. This circuit, capable of replacing a bulky passive interconnected inductor L_{passive}, consists of two small inductors (L_1, L_2), and an inverter driven by a switching frequency higher than that of the grid-connected inverter. The proposed circuit is connected in parallel to the output of the grid-connected inverter to absorb only the current ripple, thus achieving low power loss. In addition, driving the proposed circuit at a higher switching frequency than that of the conventional solution helps achieve an expanded control bandwidth while requiring a much smaller inductor.

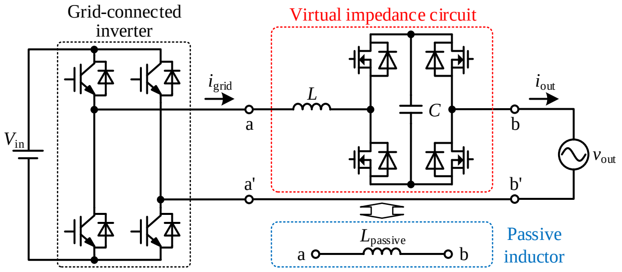

Fig. 1. Grid-connected inverter with series-type virtual impedance circuit.

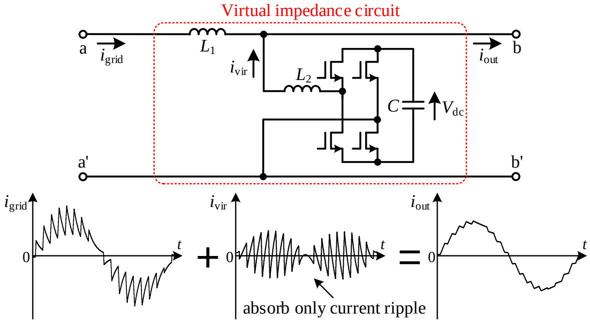

Fig. 2. Proposed parallel-type virtual impedance circuit.

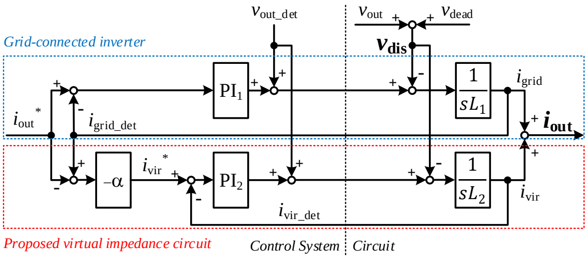

Fig. 3. Control block diagram of the proposed system.

Fig. 3 shows the control block diagram of the grid-connected inverter with the proposed virtual impedance circuit. The current controls are employed with PI controllers.

The relationship between the disturbance gain $G_{\text{dis\_conv}}$ of the grid-connected inverter and the inductance L_{passive} can be explained by the transfer function from the disturbance voltage v_{dis} to the output current i_{grid}, which is derived as follows:

$$G_{\text{dis\_conv}} = \frac{i_{\text{grid}}}{v_{\text{dis}}} = -\frac{1}{L_{\text{passive}}}\frac{s}{s^2+2\zeta_1\omega_{\text{n1}}s+\omega_{\text{n1}}^2} \qquad \cdots\cdots\cdots\cdots(1)$$

where v_{dis} is the sum of the voltage errors caused by the dead time and the output voltage, ζ_1 is the damping factor, ω_{n1} is the angular frequency of the current controller PI_1, and s is the Laplace operator. When L_{passive} is small, the THD of i_{grid} worsens, as $G_{\text{dis\_conv}}$ increases.

In contrast, the disturbance gain of the proposed system $G_{\text{dis\_pro}}$ is expressed as:

$$\begin{aligned} G_{\text{dis\_pro}} &= \frac{i_{\text{out}}}{v_{\text{dis}}} = G_{\text{dis1}} + G_{\text{dis2}}\cdot G_{\text{dis3}} \\ G_{\text{dis1}} &= -\frac{1-\alpha}{L_1}\frac{s}{s^2+2\zeta_1\omega_{\text{n1}}s+\omega_{\text{n1}}^2} \\ G_{\text{dis2}} &= -\frac{1}{L_2}\frac{s}{s^2+2\zeta_2\omega_{\text{n2}}s+\omega_{\text{n2}}^2} \\ G_{\text{dis3}} &= 1+\frac{\alpha L_2}{L_1}\frac{s^2}{s^2+2\zeta_1\omega_{\text{n1}}s+\omega_{\text{n1}}^2} \end{aligned} \qquad \cdots\cdots\cdots\cdots(2)$$

where α is the current ripple absorption ratio, L_1 and L_2 are the inductances, ζ_2 is the damping factor, and ω_{n2} is the angular frequency of the current controller PI_2.

Fig. 4 shows the comparison between the disturbance gains, $G_{\text{dis\_conv}}$ and $G_{\text{dis\_pro}}$. Note that ω_{n1} is 3000 rad/s and ω_{n2} is 90000 rad/s. The disturbance suppression performance of the proposed system improves up to 6 kHz of the disturbance frequency. From these results, it is possible to improve the output current's distortion even with a small inductor. Moreover, in the low-frequency range, $G_{\text{dis\_pro}}$ is equivalent to G_{dis1} of (2). This implies that $G_{\text{dis\_pro}}$ is equal to $G_{\text{dis\_conv}}$ when the inductance L_{passive} of (1) is expressed as:

$$L_{\text{passive}} = \frac{L_1}{1-\alpha} \qquad \cdots\cdots\cdots\cdots(3)$$

Therefore, the virtual impedance is equivalent to L_{passive} of (3), which is determined by the value of L_1 and α.

III. Experimental results of the proposed system

Fig. 5 shows the experimental waveforms of the proposed system specified in Table. 1. In this experiment, for simplicity, a DC power supply is used instead of a capacitor as in the proposed virtual impedance circuit. The THD of grid-connected inverter's output current i_{grid} is high, indicating that i_{grid} is distorted. This is because reducing the inductance L_1 leads to a decrease in the disturbance suppression performance. On the other hand, the THD of output current i_{out} with the proposed virtual impedance circuit is reduced by 65.9%.

Table. 1. Specifications of the proposed system.

Grid-connected inverter	Output power	P_{out}	800 W
	Input voltage	V_{in}	380 V
	Output voltage	V_{out}	200 V_{rms}
	Switching frequency	$f_{\text{s\_grid}}$	5 kHz
	Inductance	L_1	3 mH (%Z = 1.8%)
	Current ripple ratio of i_{out}	Δi_{out}	20%
Virtual impedance circuit	DC-link voltage	V_{dc}	380 V
	Switching frequency	$f_{\text{s\_vir}}$	150 kHz
	Inductance	L_2	500 μH (%Z = 0.3%)
	Current ripple absorption ratio of i_{grid}	α	80%

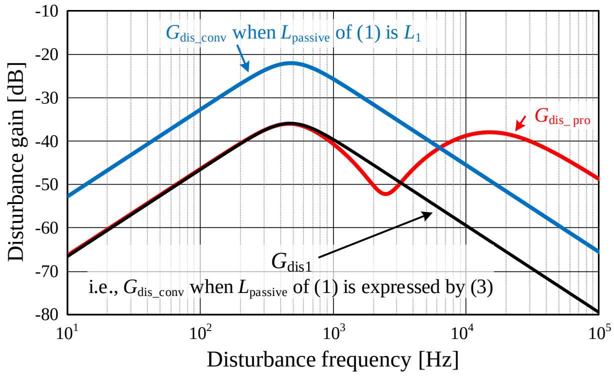

Fig. 4. Characteristics of disturbance gain.

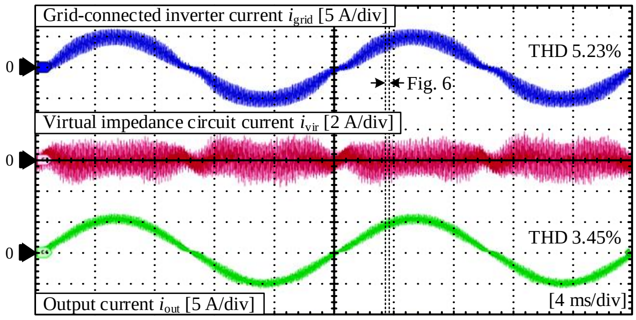

Fig. 5. Experimental waveforms of the proposed system.

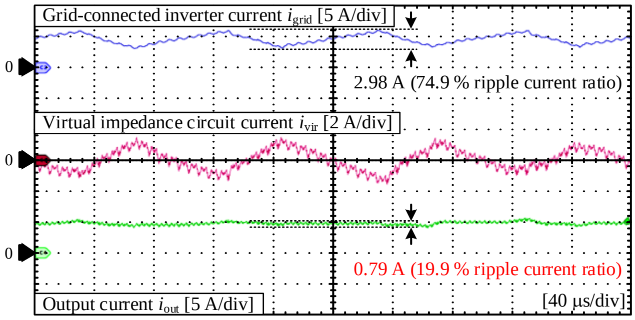

Fig. 6. Extended waveforms of the proposed system.

Fig. 6 shows the extended view of current waveforms. The current ripple of i_{grid} is 74.9% because L_1 value is small. In contrast, the current ripple of i_{out} is 19.9%, as the proposed circuit absorbs the current ripple. This demonstrates that the proposed system satisfies the design specification.

Future work involves further downsizing the interconnected inductor by operating the proposed circuit at a higher frequency of several hundred kHz.

References

[1] D. Rana, B. Hafez, P. Garg, S. Essakiappan, and P. Enjeti: "Analysis and design of active inductor as DC-link reactor for lightweight adjustable speed drive systems" in *Proc. IEEE Energy Convers. Congr. Expo.*, 2014